

Bioinformatics analysis and experiments identify CD74 as a potential immune target in ovarian carcinoma

Yixin Zhang¹, Xinhui Zhang², Li Zhang¹, Yuli Zhao¹, Sen Wang¹, Li Feng¹

¹Department of Medical Ultrasound, Shandong First Medical University, The First Affiliated Hospital of Shandong First Medical University & Shandong Provincial Qian Foshan Hospital, Shandong Medicine and Health Key Laboratory of Abdominal Medical Imaging, No.16766, Jingshi Road, Jinan, Shandong Province, China

²School of Clinical and Basic Medical Sciences, Shandong First Medical University and Shandong Academy of Medical Sciences, Jinan, China

Submitted: 9 August 2022; **Accepted:** 3 October 2022

Online publication: 4 October 2022

Arch Med Sci

DOI: <https://doi.org/10.5114/aoms/155116>

Copyright © 2022 Termedia & Banach

Corresponding author:

Li Feng MD, PhD
The First Affiliated Hospital of Shandong First Medical University and Shandong Provincial Qian Foshan Hospital
No.16766 Jingshi Road
Jinan, Shandong Province, China
Fax: +86-0531-82969995
E-mail: qfsfengli@163.com

Abstract

Introduction: Ovarian carcinoma (OC) is one of the most common malignancies in women worldwide. Immune checkpoint inhibitors are routinely used to treat OC, but with little clinical success. Here, we aimed to explore novel immune-effective biomarkers for OC management.

Material and methods: Datasets from The Cancer Genome Atlas, Genotype-Tissue Expression, and the Clinical Proteomic Tumor Analysis Consortium were used to identify hub genes significantly associated with CD8⁺ T effectors and immune checkpoint signatures and to explore the potential oncogenic role of cluster of differentiation 74 (CD74) in OC. The Immune Checkpoint Inhibitor Score (IMS) was constructed to predict immunotherapy responsiveness and prognosis. CD74 expression was further validated using immunohistochemistry in OC tissues.

Results: The yellow gene module showed a significant correlation with the CD8⁺ T effector and immune checkpoint profiles. Functional enrichment analysis showed that the yellow gene module was associated with immune response and antigen binding. Thus, IMS can accurately predict immunotherapy responsiveness and prognosis. In addition, CD74 was significantly upregulated at both the mRNA and protein levels in OC, and the high expression of the CD74 protein was related to the activation of various tumor-related pathways. Kaplan-Meier analysis showed that high CD74 expression correlated with poor prognosis in OC. Furthermore, CD74 expression remarkably correlated with inflammatory cytokines, immune cells, the tumor immune microenvironment, and immune checkpoints. Finally, CD74 expression in pericarcinomatous and cancer tissues from OC patients was verified via immunohistochemistry (IHC) analysis, which corresponded to the public database results (all $p < 0.05$).

Conclusions: CD74 may represent a novel immune biomarker to predict the prognosis of OC patients, as well as a potential therapeutic target related to immunotherapy, providing new ideas for the treatment of OC.

Key words: CD74, ovarian carcinoma, immune checkpoints, prognosis, tumor immunity.

Introduction

Ovarian carcinoma (OC) is one of the most common malignancies in women worldwide, diagnosed in over 313,000 patients each year [1]. Patients are usually diagnosed at an advanced stage and present with low

five-year survival rates [2], a high risk of reappearance [3], and high rates of side effects after treatment [4]. Many developments have been made in the treatment of OC in the past two decades, mainly involving immune checkpoint inhibitors (ICIs). To date, a wide range of ICIs have displayed significant clinical benefits in various tumor types [5]. However, ICI optimal use remains a major issue in their application [6]. Furthermore, the clinical use of ICIs in OC has had little success, with objective single-agent remission rates of approximately 6–15% in clinical trials [7, 8]. Therefore, considering the enormous financial burden and toxic effects of OC treatment, it is necessary to explore novel immune-effective biomarkers for OC management.

The programmed cell death protein 1/programmed cell death ligand 1 (PD-1/PD-L1) axis is the most important target of ICIs that can maintain immune function and downregulate the magnitude of the inflammatory response [9]. PD-L1 is expressed at elevated levels in cancer cells and tumor-infiltrating lymphocytes [10]. T cells cannot function because of the combination of PD-L1 and PD-1, thus evading the host immune system [11]. By targeting PD-1 or other immune checkpoints, inhibiting their downregulatory signaling, reversing malfunctioning states, and restoring a depleted state of T cell activity, ICIs can improve patient prognosis [12]. Progression-free survival and overall survival were most strongly associated with high levels of intra-epithelial CD8⁺ T cells in a meta-analysis of 21 OC studies [13]. This positive correlation suggests that the use of ICIs may be effective; however, surprisingly, early clinical trials suggest that their efficacy in OC remains limited. Thus, exploration of new potential immunotherapeutic targets for OC is crucial. Previous studies have explored the use of PD-L1/PD-1 expression levels, tumor neoantigen load, molecular subtypes, and microsatellite instability to predict responsiveness to immunotherapy [14, 15]. However, these methods are operationally complex, expensive, and have several unmet clinical requirements.

With the rapid development of bioinformatics technology, many tools have been developed to identify biomarkers [16]. These include weighted gene co-expression network analysis (WGCNA) and single-sample gene set enrichment analysis (ssGSEA) algorithms, which have been employed to screen numerous tumor biomarkers [17, 18]. In this study, we aimed to identify new immune therapeutic targets for OC using bioinformatic analysis combined with experiments.

Material and methods

Data retrieval

We collected data from The Cancer Genome Atlas (TCGA) OC cohort and normal ovarian data

from the Genotype-Tissue Expression (GTEx) database (downloaded from <http://xena.ucsc.edu>). The data from the two databases were merged using the R software. The TCGA cohort contained 379 OC samples, and the GTEx cohort contained 88 normal ovarian tissue samples. Demographic details, including race and ethnicity, for OC patients in the TCGA cohort were recorded (Supplementary Table S1). To facilitate data homogenization, the above sequencing samples were used with fragments per kilobase of exon model per million mapped fragment values. Open access is available to the above databases, and the study followed the data access policies and publication guidelines of these databases.

A total of 64 OC microarrays (F801401), which included 57 cases of OC and seven cases of distal ovarian tissues, were purchased from Bioaitech Company (Xian, China) and used to further validate cluster of differentiation 74 (CD74) expression and its prognostic value in OC. This study was approved by the Medical Ethics Committee of the First Affiliated Hospital of Shandong First Medical University (Shandong Provincial Qian Foshan Hospital, China).

Differentially expressed gene screening

The “limma” package in the R/Bioconductor software was used for differentially expressed gene (DEG) analysis. Differential expression was considered for an adjusted *p*-value < 0.05 (false discovery rate set at 5%) and $|\log_{2}FC| > 2$. The R package “pheatmap” [19] was applied to the results to prepare heatmaps using all DEGs.

Weighted gene co-expression network analysis construction

Using the existing literature, we obtained two gene sets for CD8⁺ T effectors and immune checkpoints constructed by Mariathan *et al.* [20, 21]. The R package “GSVA” [22] was used to perform ssGSEA to derive enrichment scores for CD8⁺ T effectors and immune checkpoints, constructing gene co-expression networks using WGCNA [23]. First, to construct the gene expression similarity matrix, a Pearson correlation coefficient between genes *i* and *j* was calculated as an absolute value using the following equation:

$$S_{ij} = |(1 + \text{cor}(x_i + y_i))/2|$$

The expression of genes *i* and *j* is represented by *i* and *j*, respectively. Additionally, a matrix of gene expression similarities was translated into an adjacency matrix. A soft threshold parameter represents the Pearson correlation coefficient for

each gene pair, β [24]. It enhances the strong and weak correlations at the index level:

$$a_{ij} = |(1 + \text{cor}(x_i + y_j))/2|^\beta$$

Genes that are representative of each module are named signature vector genes or MEs, and they indicate the overall level of gene expression within the module. This is calculated as:

$$ME = \text{princomp}(x_j^q)$$

where i represents the genes in module q and j represents the microarray sample in module q . The expression profile of genes in all samples and the ME expression profile of the signature vector gene were used to measure the identity of the genes in the module using Pearson correlation. We refer to this as module membership (MM),

$$MM_i^q = (\text{cor}x_p, ME^q)$$

where ME represents the gene i expression profile.

Analysis of functional and pathway enrichment

The yellow module genes were analyzed with a corrected p -value < 0.05 and an absolute value of log fold change > 0.5 as criteria for determining the significance of differential expression using Gene Ontology (GO) and the Kyoto Encyclopedia of Genes and Genomes (KEGG) [25, 26]. GO enrichment analysis consisted of three components: molecular function, biological process, and cellular composition. Significant enrichment of mRNA-related biological pathways was provided via KEGG analysis. The functional enrichment analysis described above was performed using the “clusterProfiler” R package, and the results were visualized using the “ggplot2” R package [27].

Construction of a single-sample immunomodulation pattern scoring system

To develop robust biomarkers for predicting OC prognosis and responsiveness, we used the ssGSEA algorithm to construct a scoring system based on mRNA expression levels in a single sample of the yellow module gene to assess the immunoregulatory patterns of individual OC patients, which we termed the Immune Checkpoint Inhibitor Score (IMS), for in depth analysis.

Prediction of response to immunotherapy and prognosis

The tumor immune dysfunction and exclusion (TIDE) algorithm is a computational approach to predict immune-checkpoint blockade (ICB) responsive-

ness using gene expression profiles [28]. The TIDE algorithm was used to validate the impact of IMS in predicting the clinical responsiveness to ICIs. Three cell types that limit T cell infiltration into tumors were assessed using the TIDE algorithm, including the M2 subtype of tumor-associated fibroblasts, myeloid-derived suppressor cells, and tumor-associated macrophages. A score for tumor immune escape was provided using two different mechanisms, including a score for dysfunction of tumor-infiltrating cytotoxic T lymphocytes (dysfunction) and their rejection by immunosuppressive factors (exclusion).

To assess the impact of CD74 expression on immunotherapy in OC patients, we calculated TIDE scores for OC patients using the TIDE website developed by Harvard University (<http://tide.dfci.harvard.edu/>).

Protein-protein interaction networks and filtering hub genes

In this study, an online tool named Search Tool of Interacting Genes (STRING, <https://string-db.org/>), which is specifically designed to predict protein-protein interactions (PPIs), was used to construct PPI networks for selected genes [29]. The construction of network models was visualized using Cytoscape (version 3.9.0, <https://cytoscape.org/>) using the STRING database, selecting genes with a score ≥ 0.4 [30]. In co-expression networks, the maximum cluster centrality (MCC) algorithm is considered the most efficient method for finding hub nodes. Furthermore, the MCC of each node was computed using the CytoHubba plug-in in Cytoscape [31]. These genes with the top 10 MCC values were considered hub genes.

GEPIA2 database and Kaplan-Meier survival curve analysis

CD74 expression in OC and normal tissues was compared using the Gene Expression Profiling Interactive Analysis (GEPIA2, <http://gepia2.cancer-pku.cn/>) online website, which contains both TCGA and GTEx database expression gene data [32]. In addition, Kaplan-Meier survival analysis (Kaplan-Meier plotter database, <http://www.kmplot.com/>) and immune cell infiltration analyses were performed.

Human Protein Atlas database analysis

The Human Protein Atlas (HPA) (<https://www.proteinatlas.org/>) is a database that provides researchers with access to large amounts of proteomic and transcriptomic data in specific human cells and tissues [33]. The immunohistochemistry (IHC) database from the HPA was used to verify the CD74 protein expression levels in normal ovary tissues and OC tissues.

Tumor Immune Single Cell Center database analysis

We gained access to OC single-cell sequencing data (OV_GSE118828) from the Tumor Immune Single Cell Center (TISCH) online database (<http://tisch.compgenpmics.org/>) [34, 35]. The database is used to categorize malignant cell, immune cell, and stromal cell hierarchical clustering. CD74 was then performed in these cells, and the results were obtained using a heatmap.

Clinical Proteomic Tumor Analysis Consortium and UALCAN database analysis

Clinical Proteomic Tumor Analysis Consortium (CPTAC) (<https://proteomics.cancer.gov/programs/cptac>) applies proteomics techniques to characterize protein composition and proteomes using mass spectrometry analysis of tumor biospecimens and quantitative identification of each tumor sample [36]. UALCAN (<http://ualcan.path.uab.edu/>) is a user-friendly online resource for analyzing publicly available cancer data [37]. In this study, we used UALCAN to analyze CD74 protein expression and its correlation with the activation of multiple tumor-related pathways based on CPTAC.

The immunohistochemistry analysis

Tissue samples were dewaxed in xylene and hydrated using different ethanol gradients. Endogenous peroxidase was inactivated with 3% hydrogen peroxide. After washing with distilled water three times for 3 min, the antigen was repaired under high pressure using citric acid antigen repair solution. The sections were then blocked with 5% goat serum in PBS and incubated overnight at 4°C with anti-human CD74 antibody (1:50, Abcam, mouse #ab9514, UK). After washing three times, the secondary antibody (1:10000, Abcam, Cat #ab205719, UK) was then used for HRP linking, followed by diaminobenzidine tetrahydrochloride (DAB) treatment (no. ZIL-9018; ZSGB-BIO, Beijing, China) and hematoxylin staining of the nuclei. The criterion for judging the staining grade of antibodies stained in cytoplasm was as follows: double-blind reading by two experienced pathologists. Integrin 1 was positively expressed as brown-yellow granules on the cytoplasm or nucleus or both; the percentage of positive cells and the intensity of the staining under a microscope were recorded using semi-quantitative judgment. The frequency of positive cells was defined as follows: 0 – less than 5%; 1 – 5–25%; 2 – 26–50%; 3 – 51–75%; and 4 – greater than 75%. The intensity was specified as follows: 0 – colorless; 1 – light yellow; 2 – brownish yellow; and 3 – brown. The staining index (values, 0–12) was determined by multiplying the score for staining intensity with the score for the frequen-

cy of positive cells. The staining index was established as follows: 0 – negative (–); 1–4 – weak (+); 5–8 – moderate (++); 9–12 – strong (+++).

Analysis of upstream and downstream regulators

We divided the 379 patients with OC into high and low CD74 expression groups based on median expression levels. A maximum threshold of 1.0 and an adjusted *p*-value under 0.05 were set as parameters for the R package “DESeq2” [38] to identify DEGs between the two groups, where a large logarithmic fold change was used. It was applied to the R packages ‘pheatmap’ [19] and ‘Enhanced-Volcano’ [39] to develop heatmaps and volcano plots. Enriched pathways were determined using gene set enrichment analysis (GSEA) [22].

c-BioPortal database analysis

Analysis of hub gene alterations in the TCGA dataset from the cBioPortal database (<http://www.cbioportal.org/>) was performed. Alterations and mutation site information for hub genes were identified using the ‘Oncoprint,’ ‘Cancer Type Summary,’ and ‘Mutations’ modules.

Statistical analysis

Bioinformatic and IHC experiment outcome analyses were implemented using R (version 4.0.5, <http://www.R-project.org>) and ImageJ software. Spearman’s correlation analysis was performed to calculate the association coefficients between the two factors. The Kaplan-Meier method was used to generate survival curves for prognostic analysis, and the log-rank test was used to determine significant differences. Multiple comparisons were adjusted for *p*-values using the false discovery rate method, with statistical significance set at *p* < 0.05 and the false discovery rate < 0.05.

Results

Research procedure

An illustrated flow diagram (Supplementary Figure S1) was produced to present the process of this study in detail.

Differentially expressed gene selection

The induction cohort consisted of 88 normal and 379 OC samples. Standardized before and after data were visualized using a box plot and examined via principal component analysis. The results showed that a total of 2253 DEGs were obtained following $|\log_{2}FC| > 2$ and a *p*-value < 0.05. The DEGs are shown in the heatmap in Supplementary Figure S2.

Weighted gene co-expression network analysis construction and key module identification

We included 379 OC samples and 88 normal samples from the GTEx cohort and selected genes with greater variance than all quartiles of variance in the different samples. In addition, all genes obtained were subjected to WGCNA, and a clustering dendrogram was used to assign these genes to seven different modules (Figure 1 A). In our study, a standard scale-free network was constructed with the Pick-Soft Threshold function by choosing $\beta = 4$ (Supplementary Figure S3). After choosing

gene expression modules related to the features of CD8⁺T effectors and immune checkpoints, the yellow gene module was found to be significantly associated with CD8⁺T effectors and immune checkpoint profiles (CD8⁺T effectors: $r = 0.77$, $p = 6e-58$; immune checkpoint: $r = 0.86$, $p = 2e-86$) (Figure 1 B), indicating that the genes contained inside the yellow module may play a critical role in the clinical success of patients. Moreover, a strong correlation was found between the number of yellow module members and the genetic characteristics of CD8⁺T effectors and immune checkpoints (CD8⁺T effectors: $r = 0.96$, $p = 8.7e-136$; immune checkpoint: $r = 0.93$, $p = 3.5e-107$) (Figures 1 C, D).

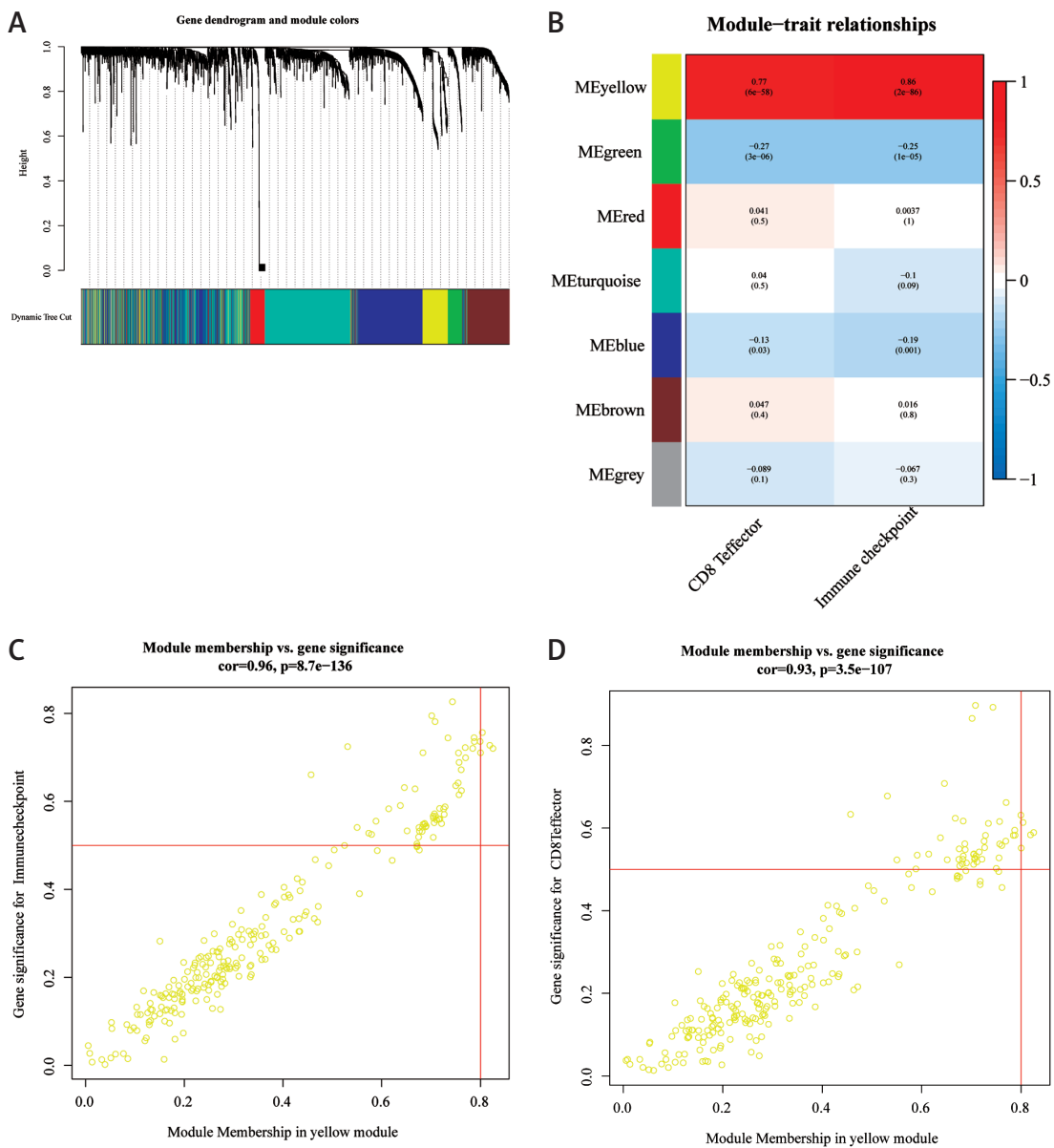


Figure 1. Co-expressed genes and module-trait relationship networks. **A** – Dendrogram of clusters based on different indicators of differentially expressed genes. Each branch of the diagram represents a gene; each color denotes a module containing a co-expressed weighted gene. **B** – Heatmap of associations between modular signature genes and CD8⁺T effectors and immune checkpoint signaling in ovarian cancer. Every column includes the corresponding p value and correlation. **C, D** – Scatterplot of the module signature genes in the yellow module

Furthermore, GO analysis indicated that genes in the yellow block were predominantly enriched for immune response, immunoglobulin complex, and antigen-binding functions (Figure 2 A, Supplementary Table SII). KEGG analysis of the yellow modular gene correlated with antigen processing and presentation, the tuberculosis pathway, Th1 and Th2 cell differentiation, and systemic lupus erythematosus (Figure 2 B, Supplementary Table SIII). The majority of these signaling pathways are involved in different core biological processes, including those related to immune regulation, and some have shown relevancy to immunotherapy [40, 41]. This demonstrates that the yellow module genes are of great importance and provide the foundation for analyzing the association between yellow gene modules and immune phenotypes.

Immune Checkpoint Inhibitor Score: a potential biological predictor

A scoring system using ssGSEA was constructed based on the individual variability and com-

plexity of the prognosis of OC patients treated with anti-PD-L1 therapy using 244 genes from the yellow gene module and quantifying the level of prognosis for each sample, which we refer to as a scoring system, IMS.

Immunotherapy responsiveness and prognosis in IMS

The TIDE algorithm was evaluated using TCGA of 379 OC samples to further assess the general applicability of IMS in predicting responsiveness to immunotherapy (Figure 3 A). We found a negative correlation between IMS and myeloid-derived suppressor cell levels and tumor-associated M2 macrophages ($r = -0.63, p < 2.2e-16$ and $r = -0.6, p < 2.2e-16$, respectively) and a positive correlation with tumor-associated fibroblast levels ($r = 0.34, p = 1.5e-11$). Moreover, there was a negative association with exclusion ($r = -0.22, p = 2.2e-05$) and a positive association between IMS and dysfunction ($r = 0.58, p < 2.2e-16$). The association between TIDE scores and IMS was strong (TIDE: $r = 0.55, p < 2.2e-16$). Ji *et al.* [28] stated

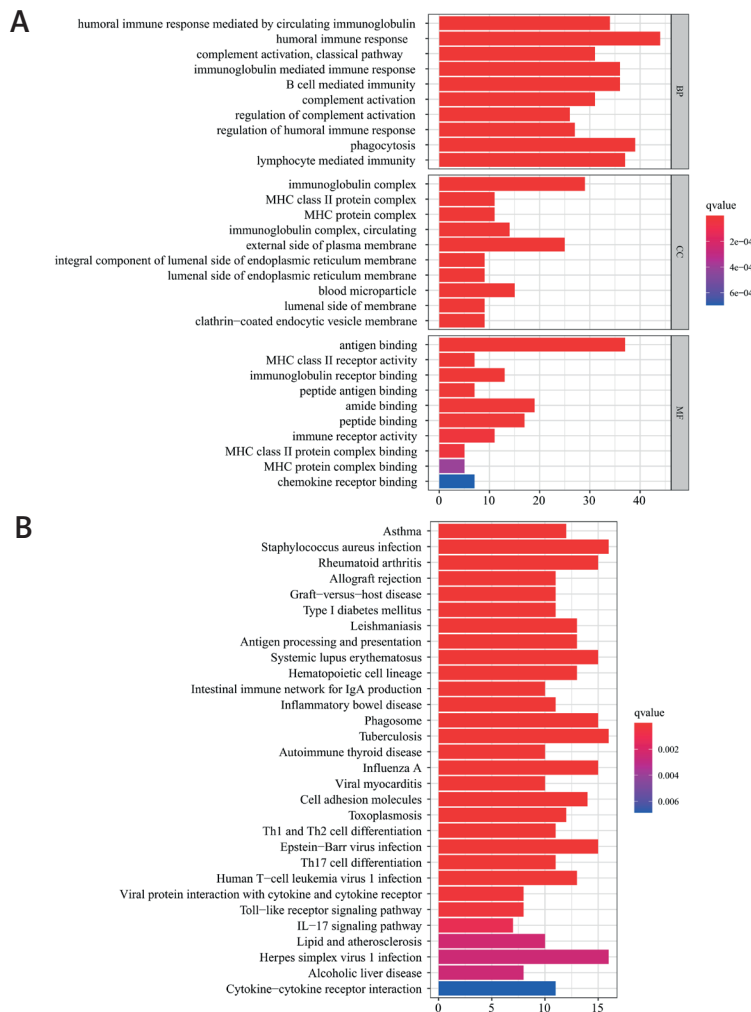


Figure 2. Analysis of Gene Ontology (A) and KEGG pathway enrichment (B) in the yellow module for genes

A

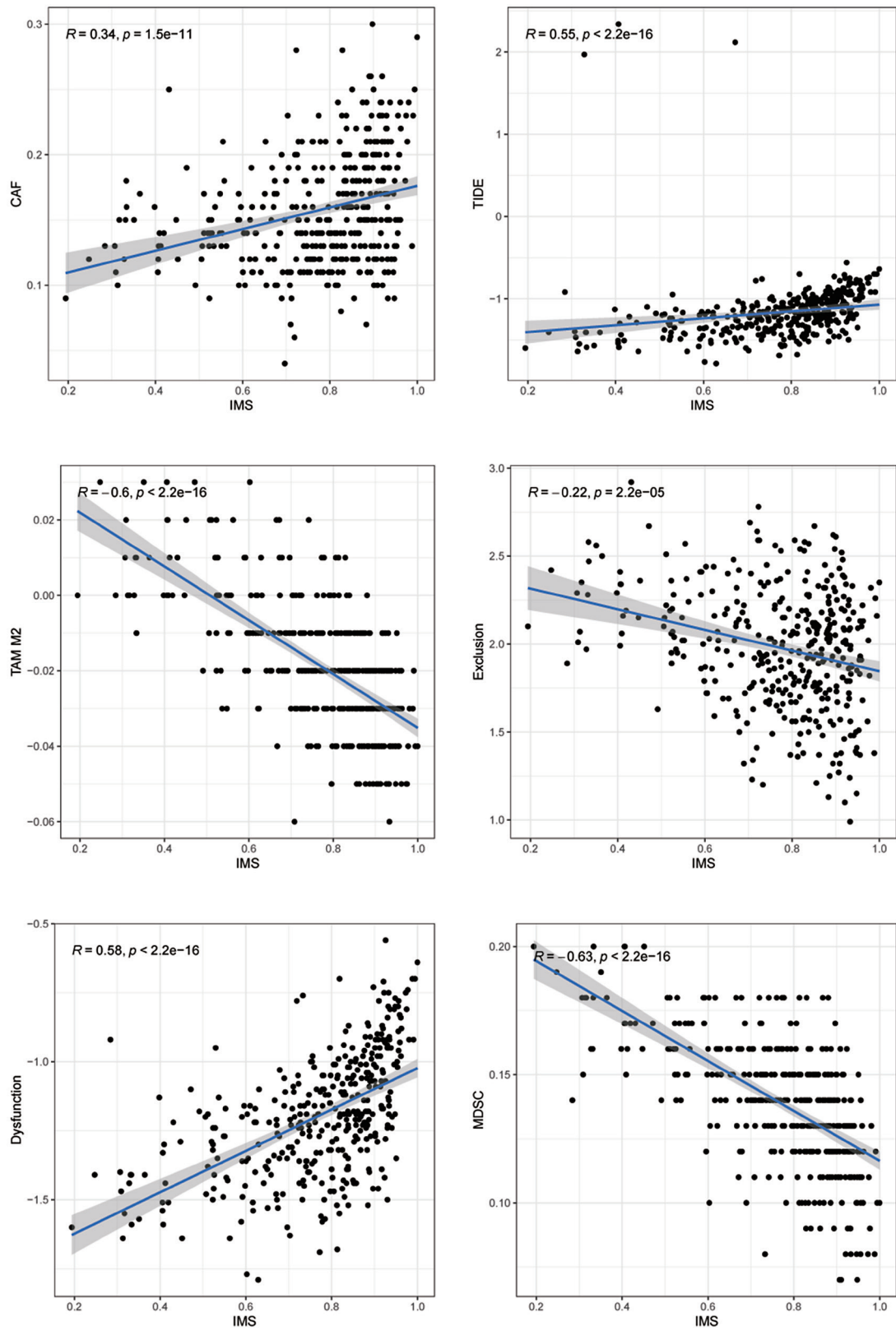


Figure 3. Immune checkpoints inhibitor score (IMS). A – An analysis of the correlation between IMS and tumor immune exclusion and dysfunction scores, involving tumor-associated fibroblasts (CAFs), M2 subtype of tumor associated macrophage (TAM), myeloid-derived suppressor cells (MDSCs), tumor-infiltrating cytotoxic T lymphocyte (CTL) dysfunction, and exclusion of CTL by immunosuppressive factors

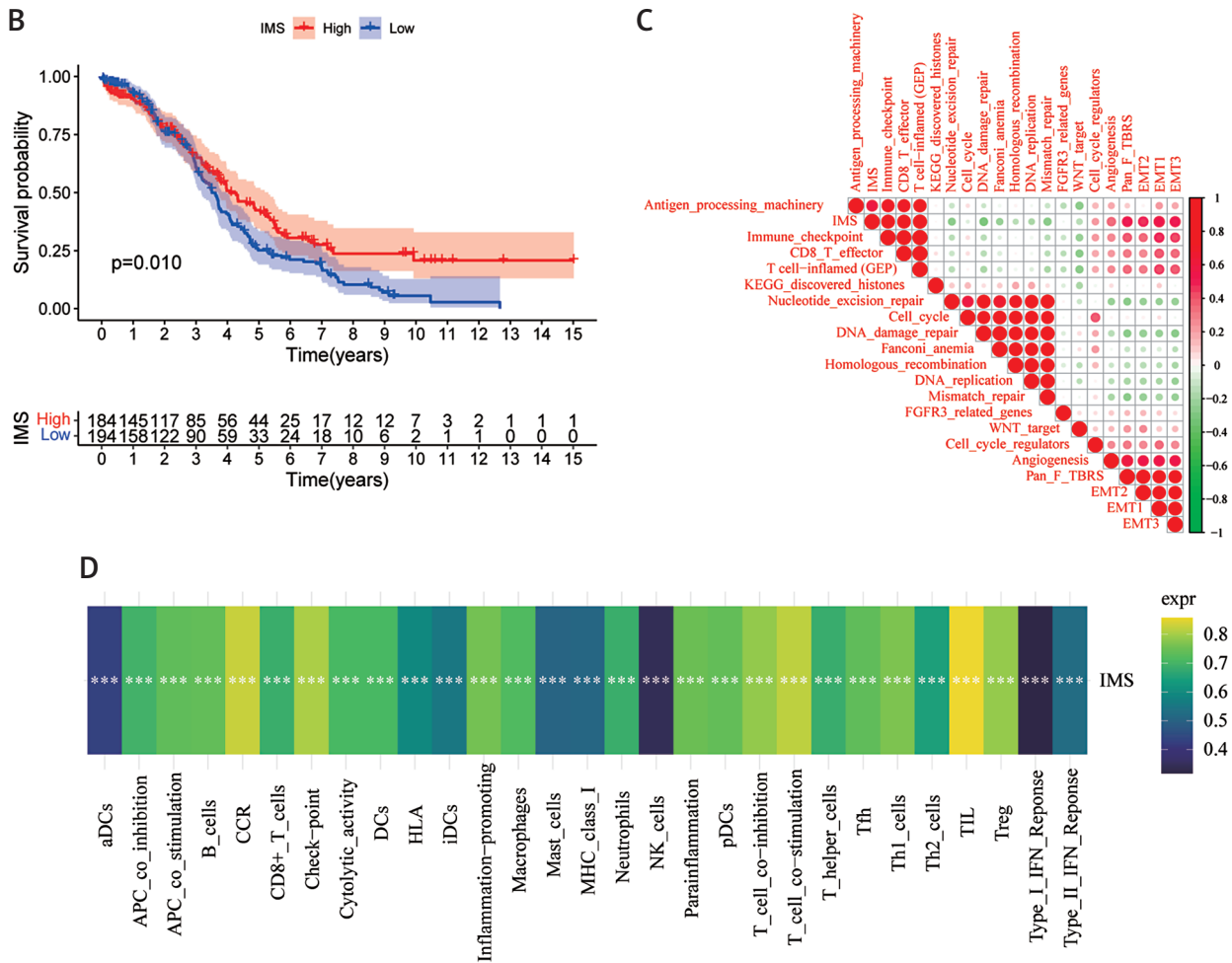


Figure 3. Cont. **B** – The Kaplan-Meier curve shows the effect of IMS on overall survival. **C** – An analysis of Spearman correlations between IMS and known genetic traits in the TCGA cohort. Red represents positive correlations and green represents negative correlations; the larger the circle, the higher the correlation. **D** – Relevance of IMS to immune cells; the asterisk represents the statistical *p* values (**p* < 0.05; ***p* < 0.01; ****p* < 0.001)

that high TIDE scores could benefit from immunotherapy, which confirms that our IMS can predict responsiveness to immunotherapy.

Based on the optimal cutoff values, we divided the IMS into high- and low-expression groups. Subsequently, we conducted an IMS survival analysis, showing the prognosis of a lower survival benefit in the low IMS cohort than in the group with anti-PD-L1 immunotherapy (*p* < 0.05, Figure 3 B). Furthermore, we linked IMS to gene scores for biologically important pathways in OC (Figure 3 C), and IMS was positively associated with antigen processing machinery, immune checkpoint, CD8⁺ T effector, EMT1, and EMT3 scores and was negatively associated with DNA damage repair and mismatch repair. In addition, we assessed the relationship between IMS and immune cells (Figure 3 D), and a positive correlation was confirmed with most immune cells (*p* < 0.001). These results further validated the positive relationship between IMS and the level

of immune cell infiltration in the tumor microenvironment.

Protein-protein interactions network construction and hub gene identification

To identify the hub genes in OC, we uploaded 244 key genes to the STRING database and constructed PPI networks under an interaction score threshold of 0.4 (Figure 4 A). The interaction data were then downloaded and imported into the Cytoscape software. The top 10 hub genes with the highest degree filtered by CytoHubba calculations were *CD74*, *HLA-DRA*, *CTSS*, *TYROBP*, *SPI1*, *C1QA*, *FCGR3A*, *FCER1G*, *C1QB*, and *C1QC* (Figure 4 B).

CD74 expression and prognostic significance in OC patients

CD74 expression was compared between OC samples and normal peritumoral tissues. Using

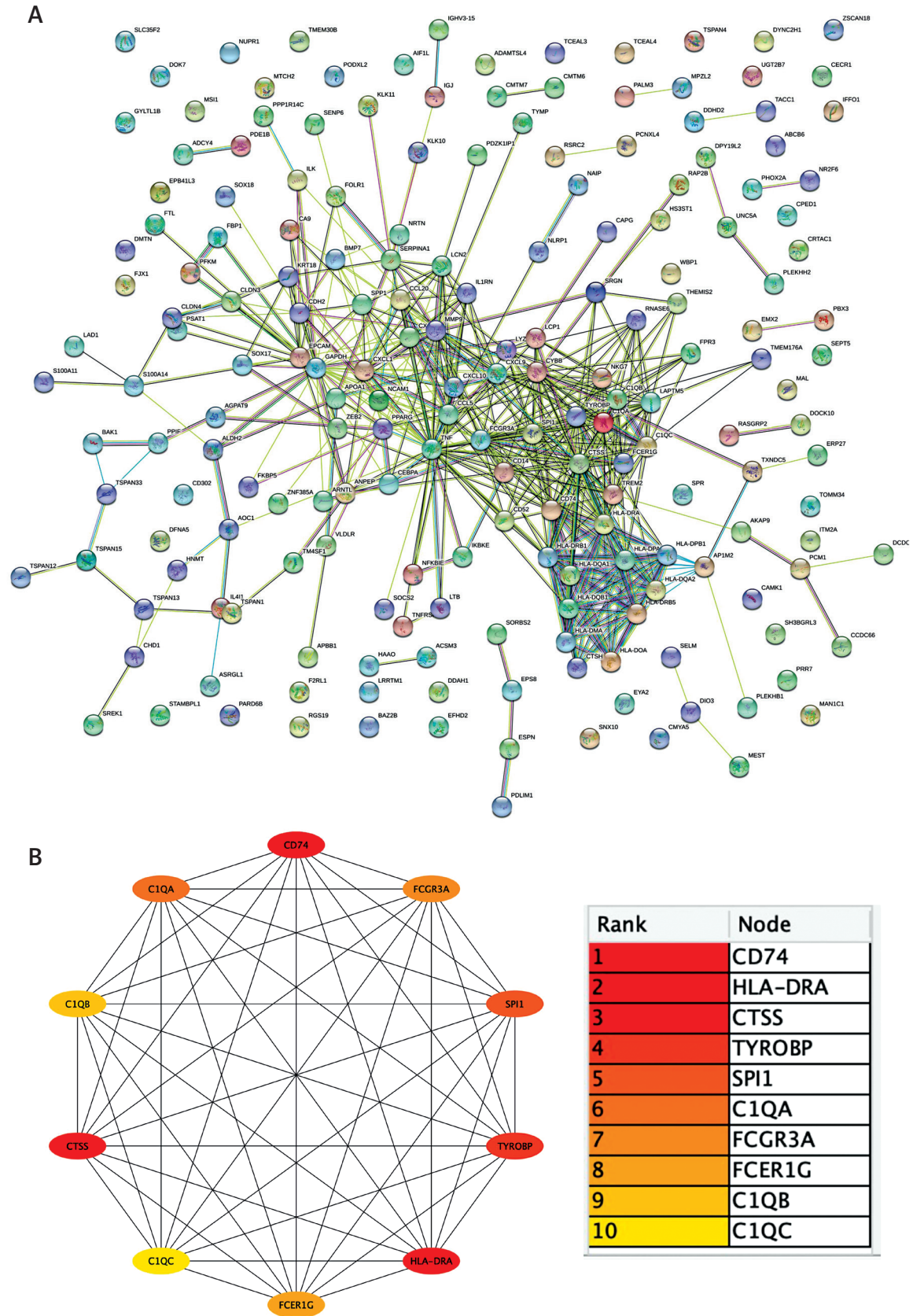


Figure 4. A – PPI network was constructed using STRING database, with interaction score 0.4. B – Top ten hub genes were ranked by maximum cluster centrality (MCC) algorithm with CytoHubba software

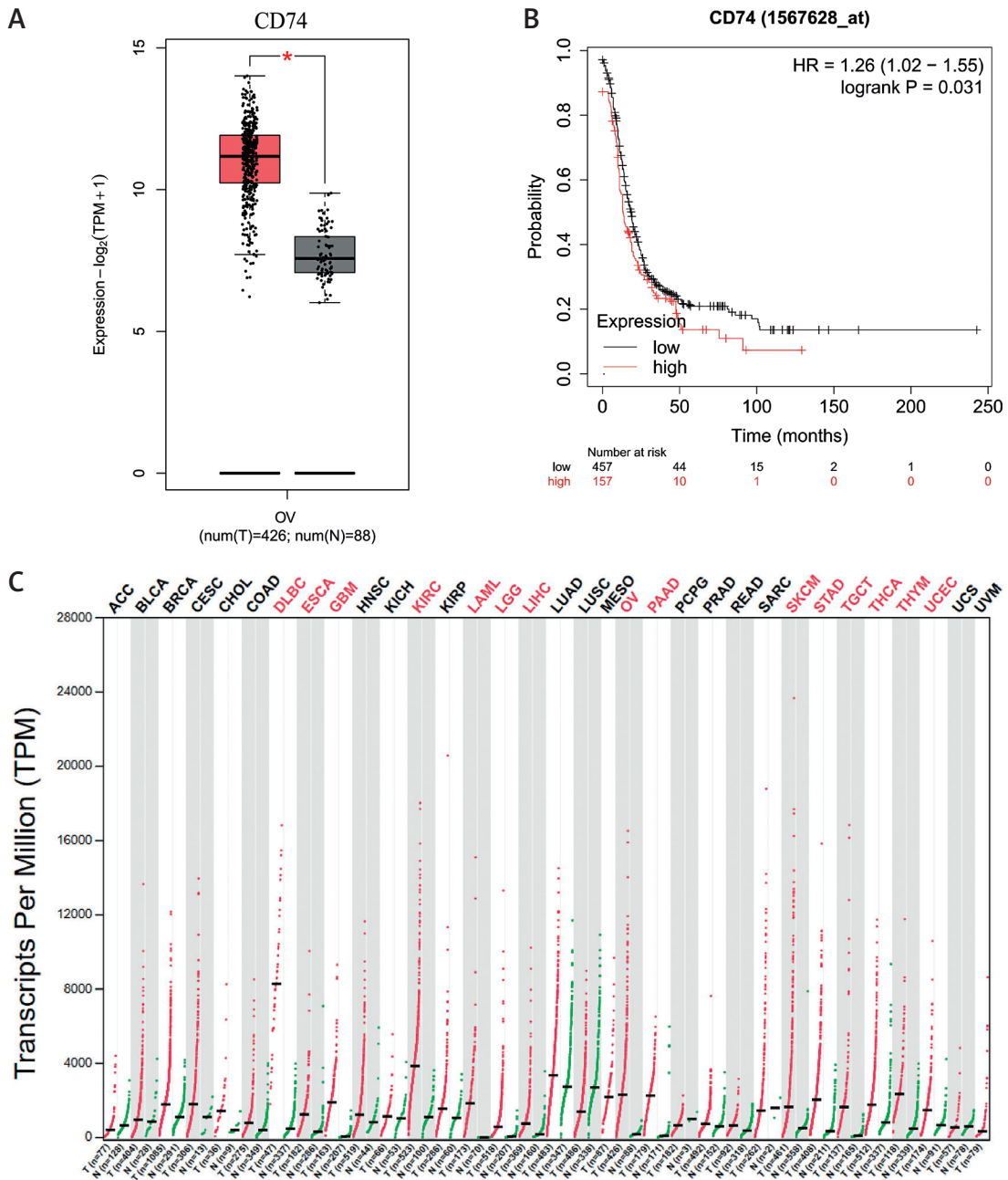


Figure 5. Data from RNA-seq of tumor tissue and normal peritumor tissue. **A** – Data from the Gene Expression Omnibus (GEO) database showed that CD74 mRNA expression was significantly higher in OV ($N = 426$) than in normal tissue ($N = 88$). **B** – Kaplan-Meier survival plot relates high expression of CD74 (Probe id = 1567628_at) to a reduced probability of progression-free survival in patients with ovarian cancer, with a hazard ratio of 1.26. **C** – Differential expression of RNA-seq in various cancers. Red indicates a difference; black represents no difference ($*p < 0.05$)

the GEPIA2 database, we observed CD74 overexpression in OC patients (Figure 5 A). Interestingly, we found that high CD74 expression was associated with poor prognosis in OC patients (Figure 5 B). The relationship between CD74 and tumorigenesis has not been well characterized. A comprehensive analysis of 33 tumors was performed to identify CD74 expression in other carcinomas. Of these tumors, 15 exhibited CD74 overexpression (Figure 5 C). Finally, we validated CD74 expression

in normal ovarian and OC tissues using the HPA database. The results showed that CD74 expression was significantly higher in tumor tissues than in normal ovarian tissues (Figure 6).

No correlation was observed between CD74 expression and cancer stage, patient race, tumor grade, TP53 mutation status, or patient age (Supplementary Figures S4 A–E). Based on TCGA data, no significant relationships were observed between patient race or ethnicity and CD74 ex-

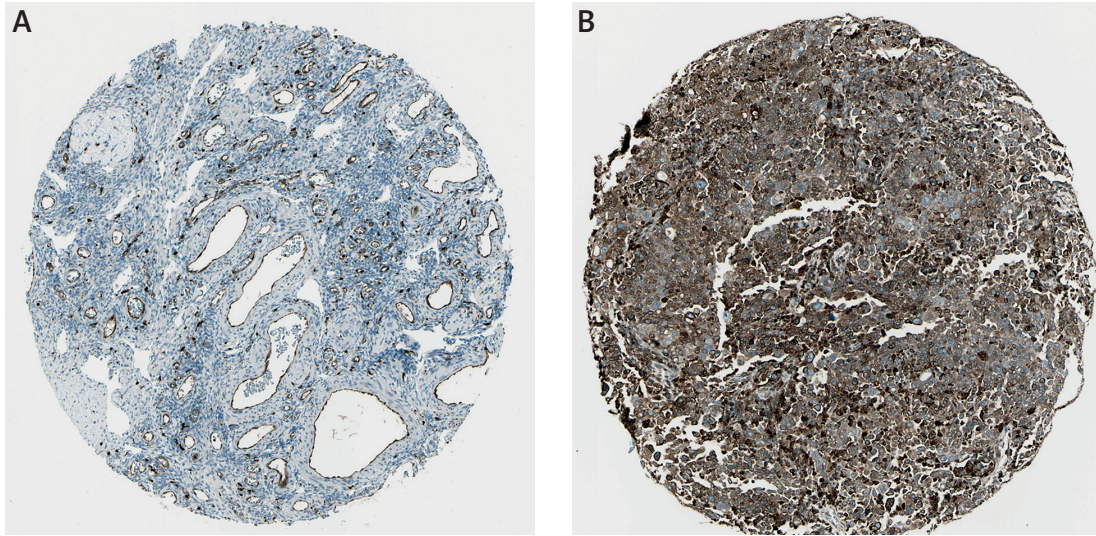


Figure 6. The Human Protein Atlas (HPA) database for immunohistochemistry of normal tissues and the CD74 gene in OC. **A** – Protein levels of CD74 in normal ovary. **B** – Protein levels of CD74 in OC tissue

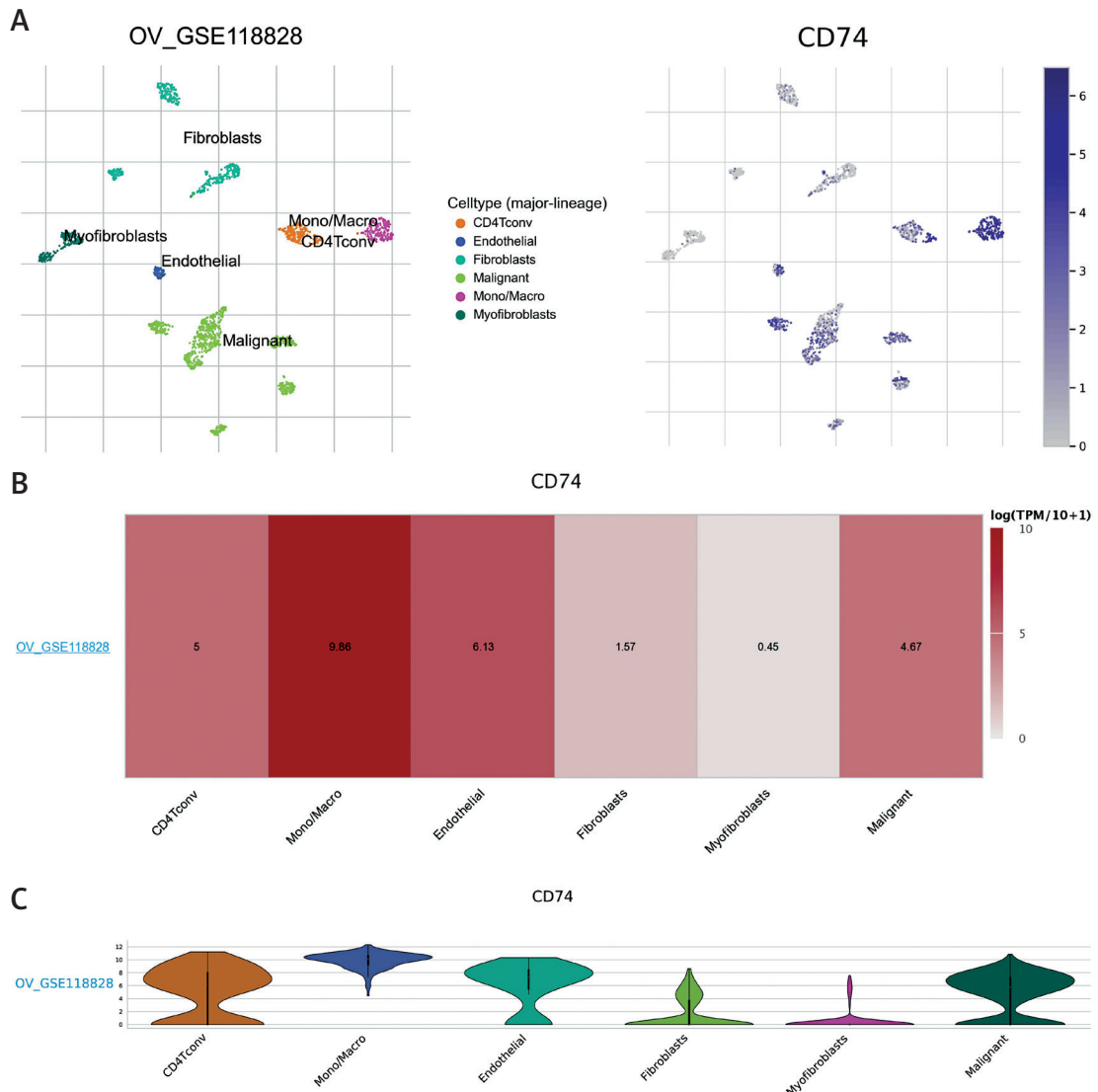


Figure 7. Association between CD74 and the tumor immune microenvironment using TISCH. **A** – Analysis of CD74 expression at the single cell level. **B** – Distribution of mean CD74 expression in different cell types. **C** – Expression distribution of CD74 in various cell types using violin plots

pression (Supplementary Figure S5). GEPIA2 data showed that expression of CD74 in patients with OC did not differ significantly between disease stages (Supplementary Figure S4 F). These findings indicate that CD74 could be used as a novel diagnostic marker in OC, regardless of the pathological parameters.

Correlation between CD74 and the tumor immune microenvironment

We used a dataset from the TISCH database (OV_GSE118828) to assess CD74 expression in tumor microenvironment-associated immune cells. Figure 7 A shows the distribution of various immune cells involved in the OV_GSE118828 database. CD74 expression levels in myofibroblasts and fibroblasts were relatively low compared to those in malignant cells and mono/macro cells in the OV_GSE118828 dataset (Figure 7 A, B). For other elements of the tumor microenvironment, relatively high levels of CD74 expression were observed in CD4⁺ T cells and endothelial cells in the dataset. A violin diagram showed the same CD74 expression trend in the microenvironment of OC cells (Figures 7 A, C). Single-cell sequencing has shown that CD74 is predominantly expressed in malignant cells, as well as in mono/macro cells in OC, and that macrophages in the tumor microenvironment are usually tumor-promoting and induce an immunosuppressive environment [42]. These results indicate that CD74 is closely related to the malignant degree of OC cells and the immune process of OC patients.

CD74 expression and immune-related genes

The relevance of CD74 to immune-related genes, such as inflammatory cytokines and immune checkpoints, was assessed to further explore CD74 profiles. A list of genes encoding inflammatory cytokines and immune checkpoints was selected from previous studies [43, 44]. The results showed that immune checkpoints, such as PD-L1, PD-1, LAG3, and CTLA4, were correlated with high expression of CD74 (Figure 8 A). In addition, some inflammatory cytokines, such as IL-10, CCL2, and IL-6 were positively correlated with CD74 expression (Figure 8 B).

Protein expression of CD74 in patients with OC

To comprehensively analyze CD74 protein expression, CPTAC was analyzed using the UALCAN database. The results demonstrated that CD74 protein expression was markedly higher in OC tissues than in normal tissues (Figure 9 A). At the same time, the results also showed that high expression of the CD74 protein was related to the activation of various tumor-related pathways (Figures 9 B–E).

CD74 expression in patients with OC

To further validate the role of CD74 in OC, we examined the protein levels of CD74 via IHC using tissue microarrays. Typical images of CD74 expression in OC tissues and corresponding para-

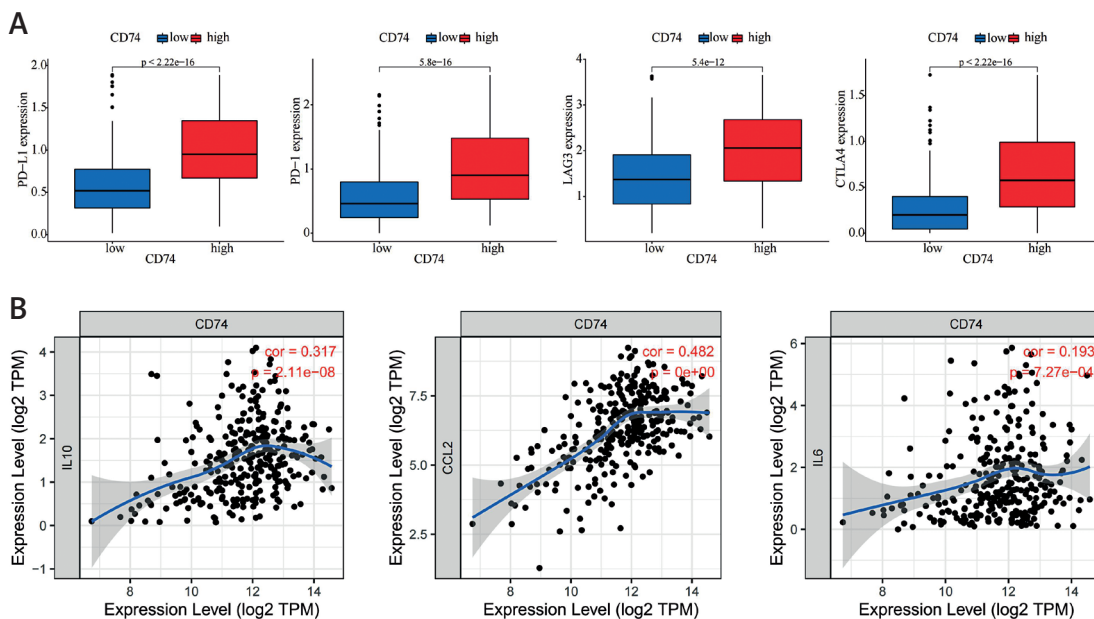


Figure 8. A – Relevance of CD74 to immune checkpoints PD-L1, PD-1, LAG3 and CTLA4. B – Correlation between CD74 and inflammatory cytokines IL-10, CCL2 and IL-6

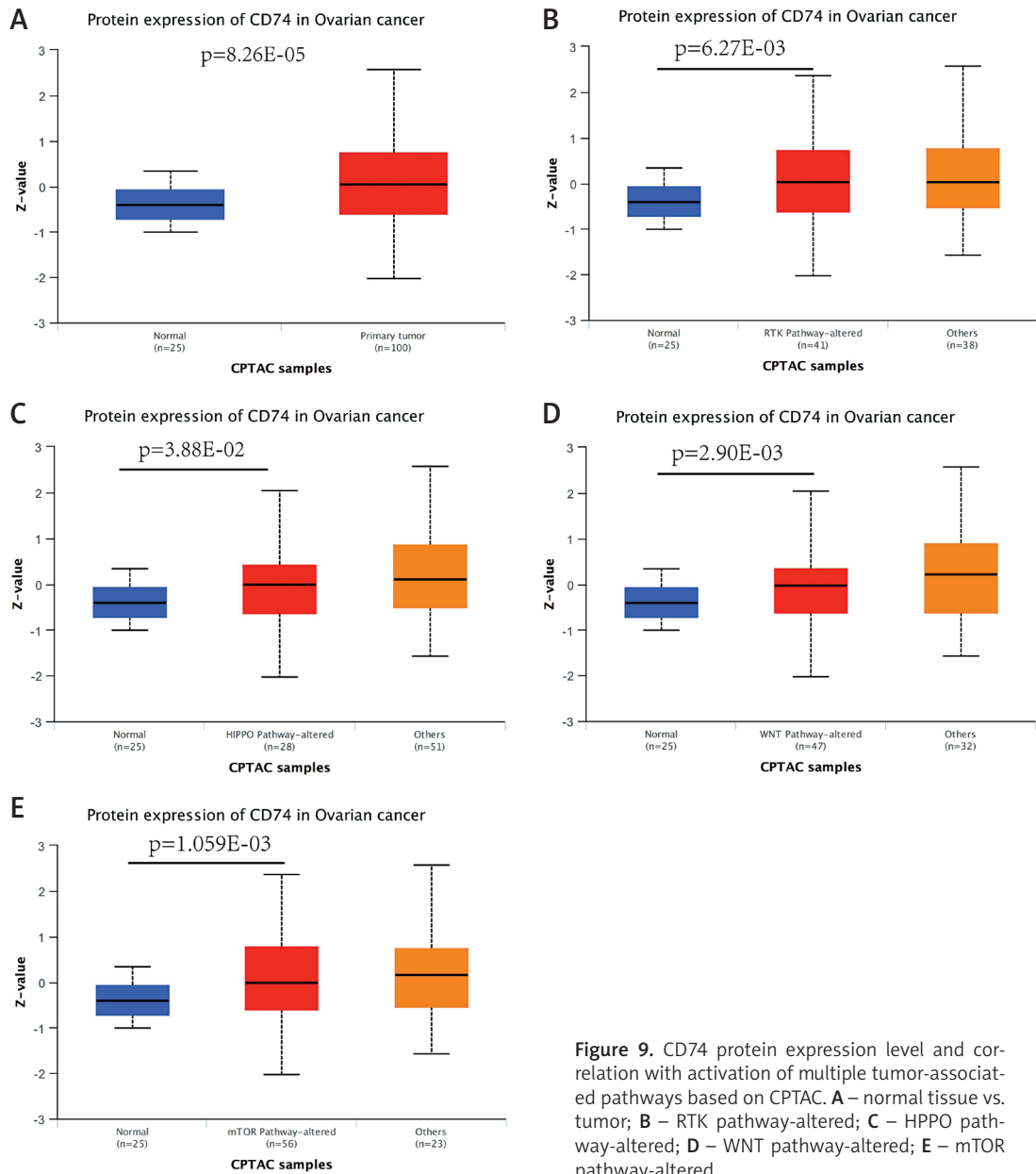


Figure 9. CD74 protein expression level and correlation with activation of multiple tumor-associated pathways based on CPTAC. **A** – normal tissue vs. tumor; **B** – RTK pathway-altered; **C** – HIPPO pathway-altered; **D** – WNT pathway-altered; **E** – mTOR pathway-altered

neoplastic tissues are shown in Figure 10 A. The findings of our study suggest that CD74 is an oncogene that is highly expressed in OC tissues, compared with para-tumor tissues ($p = 0.028$) (Figures 10 A, B).

Function enrichment analysis of CD74 in OC

We used GSEA to explore the potential cellular mechanisms of CD74 and identify DEGs between high- and low-CD74 expression groups ($|\log_{2}FC| > 1$, adjusted p -value < 0.05) (Figure 11 A, B). The GSEA results demonstrated that co-expressed genes were mainly associated with the NOD-like receptor signaling pathway and Epstein-Barr virus infection pathways (Figure 11 C). Moreover, the

top five differentially expressed regulators were significantly upregulated in OC patients when compared with levels in healthy patients (all $p < 0.05$) (Supplementary Figure S6).

Genetic alteration of CD74 in OC

We explored CD74 genomic alterations in patients with OC using TCGA, Firehose Legacy; TCGA, PanCancer Atlas; and TCGA, Nature 2011 datasets in the cBioPortal database and found that the most common genetic alterations in OC were amplification, deep deletion, and missense mutation. Moreover, genomic alterations to CD74 occurred in 1.7% of OC patients, and the frequency of major mutations in CD74 was 0.19% (TCGA, Pan-Cancer Atlas) (Figure 12 A, B). R108H alteration

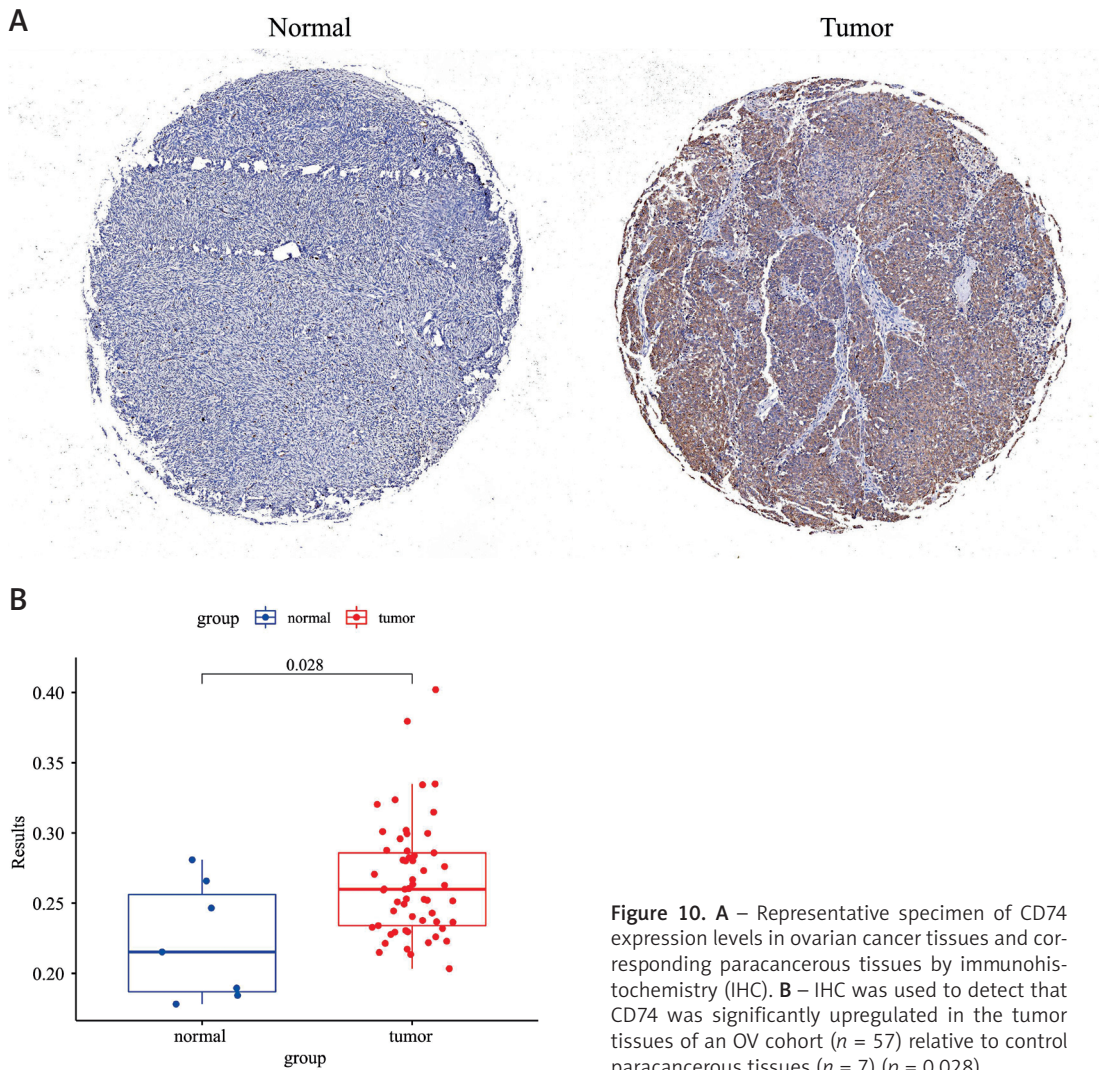


Figure 10. **A** – Representative specimen of CD74 expression levels in ovarian cancer tissues and corresponding paracancerous tissues by immunohistochemistry (IHC). **B** – IHC was used to detect that CD74 was significantly upregulated in the tumor tissues of an OV cohort ($n = 57$) relative to control paracancerous tissues ($n = 7$) ($p = 0.028$)

was detected in OC, and CD74 missense mutation was the predominant type of alteration. The most common putative copy number changes for CD74 were gain, diploid, and shallow deletion (Figure 12 C). Further information on the types, sites, and number of cases of CD74 gene modifications is shown in Figure 12 D.

Discussion

Currently, despite the widespread development of OC therapies, it remains the deadliest malignancy in women, and the prognosis for most OC patients remains dismal [45]. To date, OC has mainly been treated using surgery and chemotherapy [46]. In addition, OC is highly metastatic and invasive, and neoplasms can migrate directly into the peritoneal cavity through the peritoneal fluid, thereby spreading metastases within the peritoneal cavity and leading to deteriorating health [47]. Metastasis – the biggest obstacle in cancer treatment – has long been a research hotspot [48]. Therefore, there is an urgent need to

identify new biomarkers, particularly in the early stages, to improve the survival rate and patient quality of life. According to our analysis, CD74 was highly expressed in OC patients and strongly associated with poor patient prognosis. Moreover, a positive correlation was observed between CD74 and immune infiltration in the OC immune microenvironment. These findings suggest that CD74 could be used as a treatment for OC and as a novel biomarker for predicting the prognosis of patients with OC. Therefore, further development of CD74 as a potential target for OC treatment is essential.

In recent years, ICI therapies have rapidly changed the treatment landscape for many tumor types, resulting in unprecedented survival rates for some patients [49]. PD-1, PD-L1, CTLA-4, and other immune targets have shown effectiveness against a wide range of tumors, and immune cell activation checkpoints have proven to be the most effective activation of the antitumor immune response [50]. New ICIs, such as CD80, CD86, and

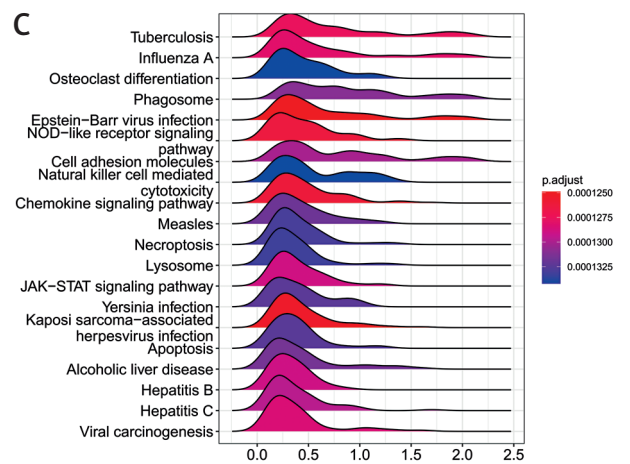
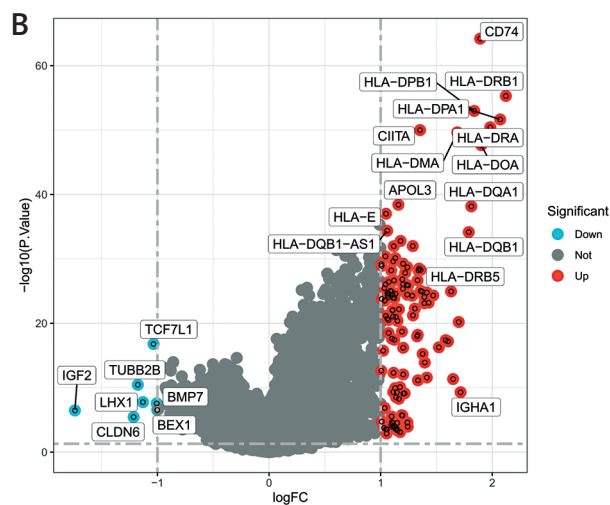
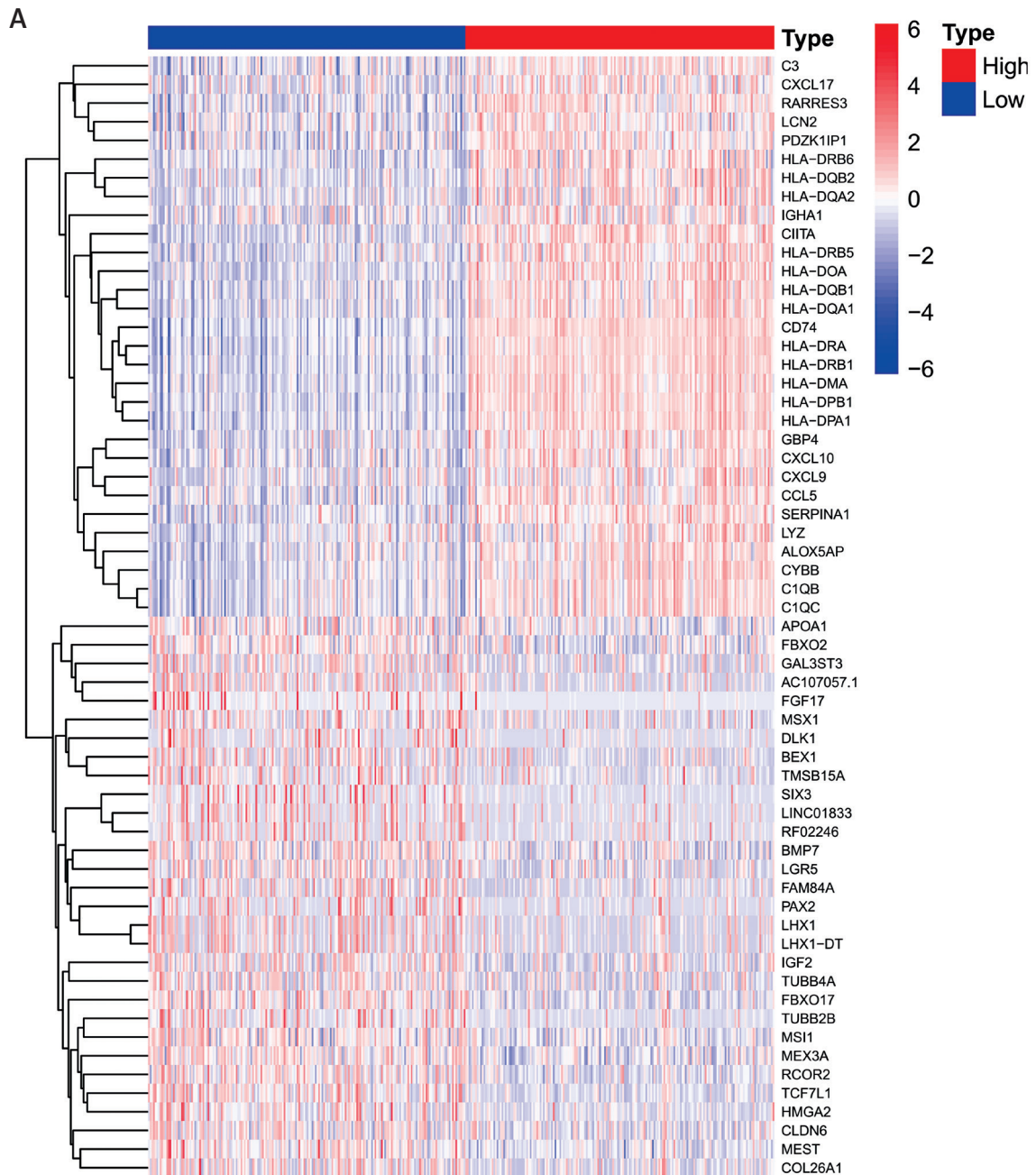


Figure 11. A – Heat map showing the top 30 differentially expressed genes (DEGs) between the high and low CD74 expression groups. **B** – Volcano plot of DEGs between the high and low CD74 expression groups. **C** – Enrichment plots from GSEA

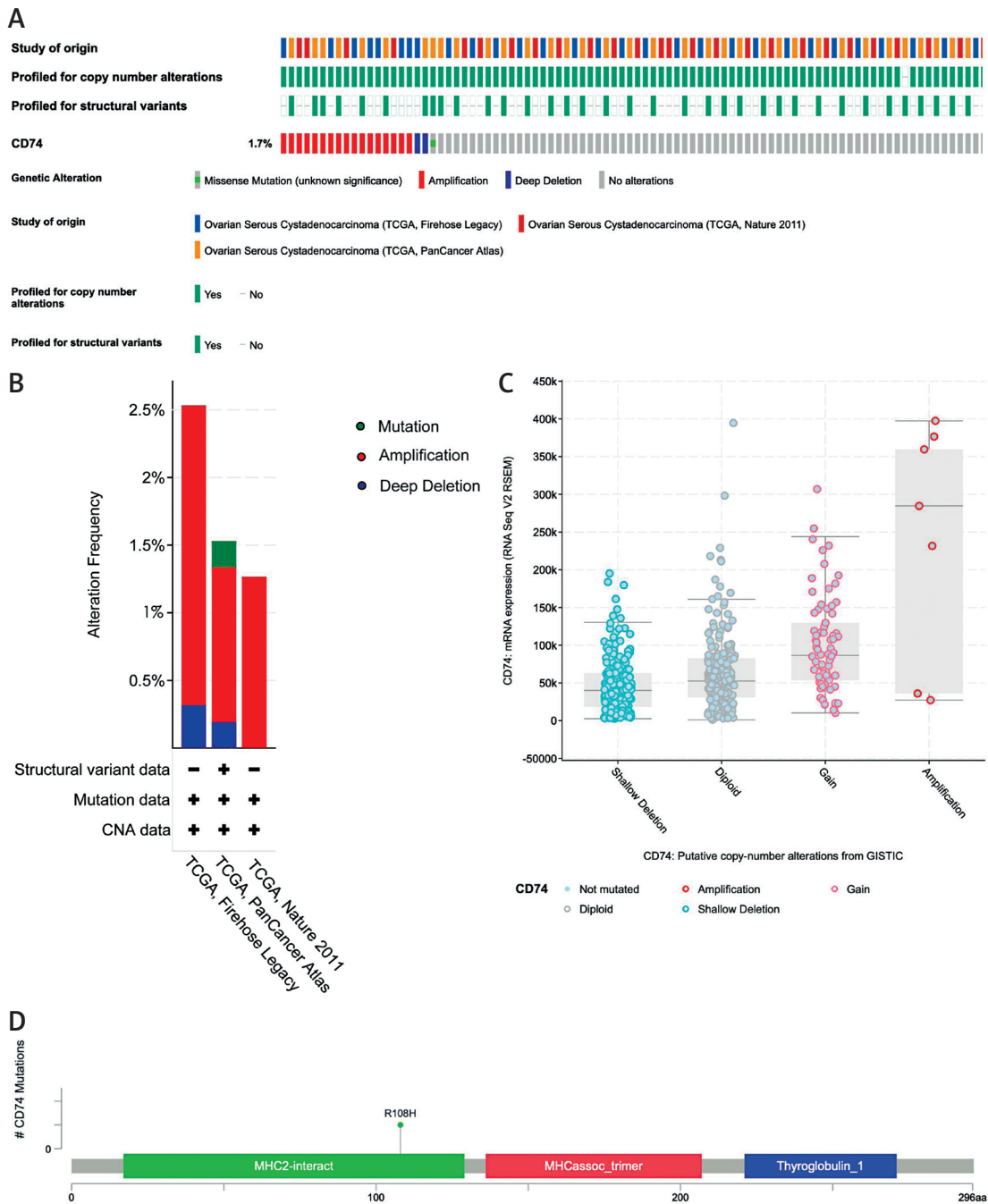


Figure 12. Genetic alteration in CD74 in OC patients. **A** – Summary of OncoPrint’s visualization of alterations to CD74 queries. **B** – Summary of CD74 alterations in OC from TCGA database. **C** – Major types of CD74 gene alterations in OC. **D** – Mutation types, number, and sites of CD74 genetic alterations

PD-L2, have been developed in recent years [51, 52]. Oncology immunotherapy has been further promoted as a research hotspot, and it has become the main treatment for some cancers. Biomarkers closely related to immunotherapy include PD-L1, PD-1, CD8⁺ T cells, and tumor mutation load. Immunotherapy is reportedly more effective in the presence of proliferating T cells [53]. Therefore, a CD8⁺ T cell-related co-expression network was constructed by estimating the proportion of CD8⁺ T lymphocytes in each sample. Gene mod-

ules with similar expression patterns were identified using WGCNA. Finally, we determined that genes in the yellow module were most closely associated with the CD8⁺ T lymphocyte content. We also constructed a scoring system to assess immunotherapy in patients with OC and found that higher IMS scores correlated with response to immunotherapy and better prognosis. Then, we selected the yellow gene model, resulting in hub genes with truly remarkable *p*-values, and CD74 expression was most prominent in hub genes.

CD74, a type II transmembrane glycoprotein, is related to the main histocompatibility complex class II alpha and beta chains and is involved in several steps in the immune system, including antigen presentation and inflammation [54]. In recent years, the role of CD74 in malignant tumors has stimulated the interest of researchers. Previous studies have shown that CD74 upregulates the ability of pancreatic cancer cells to migrate and invade via the AKT/EGR-1/GDNF signaling pathway [55]. Meanwhile, overexpression of CD74 in many other cancers, such as thyroid carcinoma and cervical carcinoma, often leads to poor patient prognosis [56, 57]. In addition, a correlation between CD74 and the immune infiltration of tumor patients has been confirmed in a variety of neoplasms. According to Noer *et al.* [58], CD74 is related to PD-L1 expression, which in turn is involved in the prevention of anti-cancer immune responses, particularly in triple-negative subtypes and metastatic breast cancer. The expression of CD74, which is also involved in glioma immune infiltration, is closely associated with the existence of multiple immune cells [59]. Our study also confirmed a correlation between CD74 and various immune cells and functions. Therefore, CD74 may serve as a novel immune biomarker of OC.

As a key element in antigen presentation, CD74 is thought to have implications in immune responses and immune infiltration. A study by Wang Z-Q *et al.* [60] showed CD74 association with poor prognosis and high tumor-infiltrating leukocytes in breast cancer, which is consistent with our findings. CD74 expression was positively correlated with the expression of immune checkpoints and inflammatory cytokines in our study. On one hand, regulating CD8⁺ T cell responses has been a central focus of immunotherapy for the treatment of cancer, as CD8⁺ T cells are the primary mediators of anti-cancer immunity [61]. Tumor-specific T cells are often dysfunctional owing to the presence of inhibitory signals at the tumor site. The elimination of these signals via immune checkpoint inhibition leads to T cell rejuvenation and clinical efficacy, although only in a small proportion of patients [62]. On the other hand, biological evidence suggests that inflammation is a hallmark of cancer [63]. Some studies have suggested that the chemokines and cytokines released by cancer and stromal cells are mediators of inflammation [64]. The activation of inflammatory cytokines can lead to cancer, including OC [65]. Next, we characterized the immunological profile of CD74 in OC patients. GO and KEGG pathway enrichment analyses indicated that CD74 positive co-expression genes were mainly enriched in immune responses and antigen processing and presentation. These

results provide preliminary evidence of the immunological properties of CD74 in OC.

The immune microenvironment also plays a significant role in cancer progression. Macrophage migration inhibitory factor (MIF) is a cell surface membrane receptor for cytokine CD74 [66]. The interactions between CD74 and MIF have been shown to play a vital role in initiating oncogenic signaling pathways that promote tumor growth and an immunosuppressive environment [67–69]. Therefore, the association between CD74 expression and the abundance of infiltrating immune cells has also been explored. Previous studies have shown that the promotion of CD74 and MIF could enhance tumor growth of pancreatic cancer and hepatocellular carcinoma in a mouse model [70, 71]. Activation of the CD74-MIF signaling pathway in the tumor microenvironment restores the antitumor activity of macrophages and dendritic cells against melanoma [69]. For further studies on the regulatory relationship between CD74 and immune cells, this analysis provides preliminary evidence of the immunological properties of CD74.

A new immunotherapy drug targeting CD74, milatuzumab, is currently undergoing clinical trials. As a membrane protein, CD74 is preferentially expressed in hematopoietic cancers and some solid tumors [72]. Twenty-five patients with relapsed or refractory multiple myeloma were treated with miralizumab infusion in a phase I multicenter clinical trial [73]. In the end, 19 patients completed treatment. Antibody-drug couples are attractive targets for CD74 therapy. Kaufman *et al.* [73] investigated the cytotoxicity of milatuzumab-doxorubicin and two milatuzumab-SN-38 couples *in vitro* and conducted *in vivo* therapeutic studies in different human cancer cell lines. Therefore, milatuzumab may be a potential therapeutic agent for various cancers. Nevertheless, little is known about the function of drugs targeting CD74 in OC. It is necessary to conduct further research in the future to discover new opportunities for treatment modalities for patients with advanced OC.

Additional experiments will contribute to a better understanding of the potential mechanisms of CD74 in OC development and progression. Although CD74 has shown involvement in a variety of immune processes, further research is needed to investigate its impact on specific immune cells.

In conclusion, the results of our bioinformatics analysis combined with experiments showed that high CD74 expression was correlated with poor prognosis and high immune infiltration in patients with OC. Therefore, CD74 could be used as a potential target for OC therapy and as a novel immune biomarker to predict the prognosis of patients with OC.

Acknowledgments

We sincerely thank the developers of the R packages and maintainers of all online public websites.

This work was funded by the National Natural Science Foundation of China (No. 31900889).

Conflict of interest

The authors declare no conflict of interest.

References

1. Sung H, Ferlay J, Siegel RL, et al. Global Cancer Statistics 2020: GLOBOCAN estimates of incidence and mortality worldwide for 36 cancers in 185 countries. *CA Cancer J Clin* 2021; 71: 209-49.
2. Menon U, Gentry-Maharaj A, Burnell M, et al. Ovarian cancer population screening and mortality after long-term follow-up in the UK Collaborative Trial of Ovarian Cancer Screening (UKCTOCS): a randomised controlled trial. *Lancet* 2021; 397: 2182-93.
3. Fabbro M, Colombo PE, Leaha CM, et al. Conditional probability of survival and prognostic factors in long-term survivors of high-grade serous ovarian cancer. *Cancers (Basel)* 2020; 12: 2184.
4. Felio J, Heredia-Soto V, Girones R, et al. Management of the toxicity of chemotherapy and targeted therapies in elderly cancer patients. *Clin Transl Oncol* 2020; 22: 457-67.
5. Yang C, Xia BR, Zhang ZC, Zhang YJ, Lou G, Jin WL. Immunotherapy for ovarian cancer: adjuvant, combination, and neoadjuvant. *Front Immunol* 2020; 11: 577869.
6. Jimenez-Sanchez A, Cybulska P, Mager KL, et al. Unraveling tumor-immune heterogeneity in advanced ovarian cancer uncovers immunogenic effect of chemotherapy. *Nat Genet* 2020; 52: 582-93.
7. Hinchcliff E, Hong D, Le H, et al. Characteristics and outcomes of patients with recurrent ovarian cancer undergoing early phase immune checkpoint inhibitor clinical trials. *Gynecol Oncol* 2018; 151: 407-13.
8. Hamanishi J, Mandai M, Ikeda T, et al. Safety and antitumor activity of anti-PD-1 antibody, nivolumab, in patients with platinum-resistant ovarian cancer. *J Clin Oncol* 2015; 33: 4015-22.
9. Yi M, Jiao D, Xu H, et al. Biomarkers for predicting efficacy of PD-1/PD-L1 inhibitors. *Mol Cancer* 2018; 17: 129.
10. Diskin B, Adam S, Cassini MF, et al. PD-L1 engagement on T cells promotes self-tolerance and suppression of neighboring macrophages and effector T cells in cancer. *Nat Immunol* 2020; 21: 442-54.
11. Ai L, Xu A, Xu J. Roles of PD-1/PD-L1 pathway: signaling, cancer, and beyond. *Adv Exp Med Biol* 2020; 1248: 33-59.
12. Hu J, Yu A, Othmane B, et al. Siglec15 shapes a non-inflamed tumor microenvironment and predicts the molecular subtype in bladder cancer. *Theranostics* 2021; 11: 3089-108.
13. Hwang WT, Adams SF, Tahirovic E, Hagemann IS, Coukos G. Prognostic significance of tumor-infiltrating T cells in ovarian cancer: a meta-analysis. *Gynecol Oncol* 2012; 124: 192-8.
14. Hasan S, Renz P, Wegner RE, et al. Microsatellite instability (MSI) as an independent predictor of pathologic complete response (PCR) in locally advanced rectal cancer: A National Cancer Database (NCDB) analysis. *Ann Surg* 2020; 271: 716-23.
15. Choucair K, Morand S, Stanbery L, Edelman G, Dworkin L, Nemunaitis J. TMB: a promising immune-response biomarker, and potential spearhead in advancing targeted therapy trials. *Cancer Gene Ther* 2020; 27: 841-53.
16. Zarabi SK, Azzato EM, Tu ZJ, et al. Targeted next generation sequencing (NGS) to classify melanocytic neoplasms. *J Cutan Pathol* 2020; 47: 691-704.
17. Yang R, Wang Z, Li J, et al. Identification and verification of five potential biomarkers related to skin and thermal injury using weighted gene co-expression network analysis. *Front Genet* 2021; 12: 781589.
18. Zhou Y, Xu B, Wu S, Liu Y. Prognostic immune-related genes of patients with Ewing's sarcoma. *Front Genet* 2021; 12: 669549.
19. Kolde R. Pheatmap: pretty heatmaps. R package version 1.0.12. 2019.
20. Mariathasan S, Turley SJ, Nickles D, et al. TGFbeta attenuates tumour response to PD-L1 blockade by contributing to exclusion of T cells. *Nature* 2018; 554: 544-8.
21. Chen Y, Tian D, Chen X, et al. ARRDC3 as a diagnostic and prognostic biomarker for epithelial ovarian cancer based on data mining. *Int J Gen Med* 2021; 14: 967-81.
22. Subramanian A, Tamayo P, Mootha VK, et al. Gene set enrichment analysis: a knowledge-based approach for interpreting genome-wide expression profiles. *Proc Natl Acad Sci U S A* 2005; 102: 15545-50.
23. Langfelder P, Horvath S. WGCNA: an R package for weighted correlation network analysis. *BMC Bioinformatics* 2008; 9: 559.
24. Horvath S, Zhang B, Carlson M, et al. Analysis of oncogenic signaling networks in glioblastoma identifies ASPM as a molecular target. *Proc Natl Acad Sci USA* 2006; 103: 17402-7.
25. Gene Ontology Consortium: going forward. *Nucleic Acids Res* 2015; 43 (Database issue): D1049-56.
26. Kanehisa M, Goto S. KEGG: Kyoto Encyclopedia of Genes and Genomes. *Nucleic Acids Res* 2000; 28: 27-30.
27. Yu G, Wang LG, Han Y, He QY. clusterProfiler: an R package for comparing biological themes among gene clusters. *OMICS* 2012; 16: 284-7.
28. Jiang P, Gu S, Pan D, et al. Signatures of T cell dysfunction and exclusion predict cancer immunotherapy response. *Nat Med* 2018; 24: 1550-8.
29. Szklarczyk D, Gable AL, Lyon D, et al. STRING v11: protein-protein association networks with increased coverage, supporting functional discovery in genome-wide experimental datasets. *Nucleic Acids Res* 2019; 47 (D1): D607-13.
30. Shannon P, Markiel A, Ozier O, et al. Cytoscape: a software environment for integrated models of biomolecular interaction networks. *Genome Res* 2003; 13: 2498-504.
31. Chin HC, Chen SH, Wu HH, Ho CW, Ko MT, Lin CY. cytoHubba: identifying hub objects and sub-networks from complex interactome. *BMC Syst Biol* 2014; 8 (Suppl. 4): S11.
32. Tang Z, Li C, Kang B, Gao G, Li C, Zhang Z. GEPIA: a web server for cancer and normal gene expression profiling and interactive analyses. *Nucleic Acids Res* 2017; 45 (W1): W98-102.
33. Thul PJ, Lindskog C. The human protein atlas: a spatial map of the human proteome. *Protein Sci* 2018; 27: 233-44.
34. Sun D, Wang J, Han Y, et al. TISCH: a comprehensive web resource enabling interactive single-cell transcriptome

- visualization of tumor microenvironment. *Nucleic Acids Res* 2021; 49 (D1): D1420-30.
35. Neftel C, Laffy J, Filbin MG, et al. An integrative model of cellular states, plasticity, and genetics for glioblastoma. *Cell* 2019; 178: 835-849.e821.
 36. Edwards NJ, Oberti M, Thangudu RR, et al. The CPTAC data portal: a resource for cancer proteomics research. *J Proteome Res* 2015; 14: 2707-13.
 37. Chandrashekar DS, Bashel B, Balasubramanya SAH, et al. UALCAN: a portal for facilitating tumor subgroup gene expression and survival analyses. *Neoplasia* 2017; 19: 649-58.
 38. Love MI, Huber W, Anders S. Moderated estimation of fold change and dispersion for RNA-seq data with DESeq2. *Genome Biol* 2014; 15: 550.
 39. Blighe K. EnhancedVolcano: publication-ready volcano plots with enhanced colouring and labeling. 2019; <https://bioconductor.riken.jp/packages/3.8/bioc/vignettes/EnhancedVolcano/inst/doc/EnhancedVolcano.html>.
 40. Flannagan RS, Jaumouille V, Grinstein S. The cell biology of phagocytosis. *Annu Rev Pathol* 2012; 7: 61-98.
 41. de Jong NWM, van Kessel KPM, van Strijp JAG. Immune evasion by *Staphylococcus aureus*. *Microbiol Spectr* 2019; 7. doi: 10.1128/microbiolspec.GPP3-0061-2019.
 42. Najafi M, Goradel NH, Farhood B, et al. Macrophage polarity in cancer: a review. *J Cell Biochem* 2019; 120: 2756-65.
 43. Wang KY, Huang RY, Tong XZ, et al. Molecular and clinical characterization of TMEM71 expression at the transcriptional level in glioma. *CNS Neurosci Ther* 2019; 25: 965-75.
 44. Xu S, Tang L, Dai G, Luo C, Liu Z. Expression of m6A regulators correlated with immune microenvironment predicts therapeutic efficacy and prognosis in gliomas. *Front Cell Dev Biol* 2020; 8: 594112.
 45. Chandra A, Pius C, Nabeel M, et al. Ovarian cancer: current status and strategies for improving therapeutic outcomes. *Cancer Med* 2019; 8: 7018-31.
 46. Marchetti C, De Felice F, Di Pinto A, et al. Dose-dense weekly chemotherapy in advanced ovarian cancer: an updated meta-analysis of randomized controlled trials. *Crit Rev Oncol Hematol* 2018; 125: 30-4.
 47. Yousefi M, Dehghani S, Nosrati R, et al. Current insights into the metastasis of epithelial ovarian cancer – hopes and hurdles. *Cell Oncol (Dordr)* 2020; 43: 515-38.
 48. Wang Y, Zhu Z. Oridonin inhibits metastasis of human ovarian cancer cells by suppressing the mTOR pathway. *Arch Med Sci* 2019; 15: 1017-27.
 49. Schoenfeld AJ, Hellmann MD. Acquired resistance to immune checkpoint inhibitors. *Cancer Cell* 2020; 37: 443-55.
 50. Rotte A. Combination of CTLA-4 and PD-1 blockers for treatment of cancer. *J Exp Clin Cancer Res* 2019; 38: 255.
 51. Wennhold K, Thelen M, Lehmann J, et al. CD86 + antigen-presenting B cells are increased in cancer, localize in tertiary lymphoid structures, and induce specific T-cell responses. *Cancer Immunol Res* 2021; 9: 1098-108.
 52. Sugiura D, Maruhashi T, Okazaki I-M, et al. Restriction of PD-1 function by cis-PD-L1/CD80 interactions is required for optimal T cell responses. *Science* 2019; 364: 558-66.
 53. Kallies A, Zehn D, Utzschneider DT. Precursor exhausted T cells: key to successful immunotherapy? *Nat Rev Immunol* 2020; 20: 128-36.
 54. Borghese F, Clanchy FIL. CD74: an emerging opportunity as a therapeutic target in cancer and autoimmune disease. *Expert Opin Ther Targets* 2011; 15: 237-51.
 55. Zhang JF, Tao LY, Yang MW, et al. CD74 promotes perineural invasion of cancer cells and mediates neuroplasticity via the AKT/EGR-1/GDNF axis in pancreatic ductal adenocarcinoma. *Cancer Lett* 2021; 508: 47-58.
 56. Cheng SP, Liu CL, Chen MJ, et al. CD74 expression and its therapeutic potential in thyroid carcinoma. *Endocr Relat Cancer* 2015; 22: 179-90.
 57. Balakrishnan CK, Tye GJ, Balasubramaniam SD, Kaur G. CD74 and HLA-DRA in cervical carcinogenesis: potential targets for antitumour therapy. *Medicina (Kaunas)* 2022; 58: 190.
 58. Noer JB, Talman MM, Moreira JMA. HLA class II histocompatibility antigen gamma chain (CD74) expression is associated with immune cell infiltration and favorable outcome in breast cancer. *Cancers (Basel)* 2021; 13: 6179.
 59. Xu S, Li X, Tang L, Liu Z, Yang K, Cheng Q. CD74 Correlated With Malignancies and Immune Microenvironment in Gliomas. *Front Mol Biosci* 2021; 8: 706949.
 60. Wang Z-Q, Milne K, Webb JR, Watson PH. CD74 and intratumoral immune response in breast cancer. *Oncotarget* 2017; 8: 12664-74.
 61. Waldman AD, Fritz JM, Lenardo MJ. A guide to cancer immunotherapy: from T cell basic science to clinical practice. *Nat Rev Immunol* 2020; 20: 651-68.
 62. Sharpe AH, Pauken KE. The diverse functions of the PD1 inhibitory pathway. *Nat Rev Immunol* 2018; 18: 153-67.
 63. Greten FR, Grivnenkov SI. Inflammation and cancer: triggers, mechanisms, and consequences. *Immunity* 2019; 51: 27-41.
 64. Nowak M, Janas L, Soja M, et al. Chemokine expression in patients with ovarian cancer or benign ovarian tumors. *Arch Med Sci* 2022; 18: 682-9.
 65. Bouras E, Karhunen V, Gill D, et al. Circulating inflammatory cytokines and risk of five cancers: a Mendelian randomization analysis. *BMC Med* 2022; 20: 3.
 66. Farr L, Ghosh S, Moonah S. Role of MIF cytokine/CD74 receptor pathway in protecting against injury and promoting repair. *Front Immunol* 2020; 11: 1273.
 67. Gai JW, Wahafu W, Song L, et al. Expression of CD74 in bladder cancer and its suppression in association with cancer proliferation, invasion and angiogenesis in HT-1376 cells. *Oncol Lett* 2018; 15: 7631-8.
 68. Zheng YX, Yang M, Rong TT, et al. CD74 and macrophage migration inhibitory factor as therapeutic targets in gastric cancer. *World J Gastroenterol* 2012; 18: 2253-61.
 69. Figueiredo CR, Azevedo RA, Mousdell S, et al. Blockade of MIF-CD74 signalling on macrophages and dendritic cells restores the antitumour immune response against metastatic melanoma. *Front Immunol* 2018; 9: 1132.
 70. Wirtz TH, Saal A, Bergmann I, et al. Macrophage migration inhibitory factor exerts pro-proliferative and anti-apoptotic effects via CD74 in murine hepatocellular carcinoma. *Br J Pharmacol* 2021; 178: 4452-67.
 71. Wen Y, Cai W, Yang J, et al. Targeting macrophage migration inhibitory factor in acute pancreatitis and pancreatic cancer. *Front Pharmacol* 2021; 12: 638950.
 72. Berkova Z, Tao R-H, Samaniego F. Milatuzumab – a promising new immunotherapeutic agent. *Expert Opin Investig Drugs* 2010; 19: 141-9.
 73. Kaufman JL, Niesvizky R, Stadtmauer EA, et al. Phase I, multicentre, dose-escalation trial of monotherapy with milatuzumab (humanized anti-CD74 monoclonal antibody) in relapsed or refractory multiple myeloma. *Br J Haematol* 2013; 163: 478-86.